MAGNETOHYDRODYNAMICS Vol. 47 (2011), No. 4, pp. 461–473

NUMERICAL MODELLING OF FREE SURFACE DYNAMICS OF MELT IN AN ALTERNATE ELECTROMAGNETIC FIELD

S. Spitans[1], *A. Jakovičs*[1], *E. Baake*[2], *B. Nacke*[2],

[1] *Laboratory for Mathematical Modelling of Environmental and Technological Processes, University of Latvia*
8 Zellu str., LV-1002 Riga, Latvia
[2] *Institute of Electrotechnology Leibniz, University of Hannover*
Wilhelm-Busch-Str. 4, D-30167 Hannover, Germany

In this work, the recently presented model for the calculation of free surface dynamics of the melt in the induction crucible furnace in a simplified two-dimensional axisymmetric consideration is further verified. The developed model is applied to the case of electromagnetic levitation, and the very first results are presented. The two-dimensional model is generalized for three-dimensional consideration as well, and on the basis of the obtained calculation results the phenomenon of free surface wave propagation along the crucible wall is discussed.

Introduction. Induction furnaces, which ensure contactless control of electromagnetic (EM) alloy stirring, temperature and free surface shape, are widely applied in metallurgical industry.

In large induction crucible furnaces (ICF), the melt is usually covered with a slag layer, which acts both as a thermal and a chemical insulator. Free surface deformations can cause slag displacement and lead to undesirable contact between the melt and the atmosphere accompanied by chemical reactions and thermal losses.

Metallic material properties are usually varied by dopant impurities that normally are scattered on the melt free surface during the stirring process. Because of the meniscus shape, light particles stay on the free surface and gather near the crucible wall. The time, at which they are forced into the melt volume, is dependent on the flow pattern and meniscus shape. Optimization of the free surface shape appears to be essential in terms of energy performance, system overheating and particle homogenization.

In case of higher power densities (e.g., an induction furnace with a cold crucible), the EM pressure squeezes the melt, and semilevitation is achieved. In this case, the melt is fully abutted upon the skull. Moreover, for reactive alloys of high purity, the furnace design leads to complete alloy levitation in a non-reactive atmosphere. At the same time, the behaviour of the free surface might be notably unsteady due to operational parameter change, mean flow instabilities and high values of turbulence kinetic energy.

Mass transfer in induction furnaces, considering the free surface dynamics [1], as well as the EM levitation phenomena [2] have been actively studied numerically.

Since the problem of free surface shape control appears to be significant for metallic materials processing, the development of models for free surface dynamics calculation remains relevant.

1. 2D model verification. In the recent work [3], the model for free surface dynamics calculation in a simplified two-dimensional (2D) axisymmetric consideration has been developed. The calculation was performed using ANSYS Classic for the EM problem, ANSYS/CFX for the hydrodynamic (HD) problem and their external coupler (V. Geza, University of Latvia). The Volume of Fluid (VOF) numerical technique in combination with the k-ω SST turbulence description was applied to calculate the two-phase flow. Due to the low magnetic Reynolds number, the EM and HD parts of the complicated magnetohydrodynamic (MHD) problem were solved separately. Moreover, because of much longer inertia times of the melt if compared to the alternate EM field timescale, only the stationary part of the Lorentz force was taken into account.

The verification of the free surface oscillation period T in case of small amplitude oscillations according to the analytical formula [4] approves the model accuracy.

The 2D hydrodynamic model results for the quasi-steady state meniscus were also compared with the calculation results of other models: self-developed 2D hydrostatic [3], the model of M. Kirpo [5] and O. Pesteanu [1] as well as with appropriate experimental measurements [5] in a *big* laboratory scale ICF setup (Fig. 1). The previous comparison has revealed an insufficient agreement and initiated further investigations of model deficiencies.

	big ICF	*small* ICF
h_{cru} mm	756	383
h_{ind} mm	570	235
R_{alloy} mm	158	85
R_{ind} mm	196.5	100
inductor turns N	11 (lower switched off)	12
Non-magnetic materials specific resistivity [Ω·m]		
Copper inductor $\rho_{\mathrm{Cu}} = 0.2 \cdot 10^{-7}$	Steel crucible $\rho_{\mathrm{Fe}} = 0.7 \cdot 10^{-6}$	Wood's metal alloy $\rho_{\mathrm{Wm}} = 1.0 \cdot 10^{-6}$
Wood's metal:		
$\rho = 9400\,\mathrm{kg/m^3}$		$\eta = 0.0042\,\mathrm{Pas}$

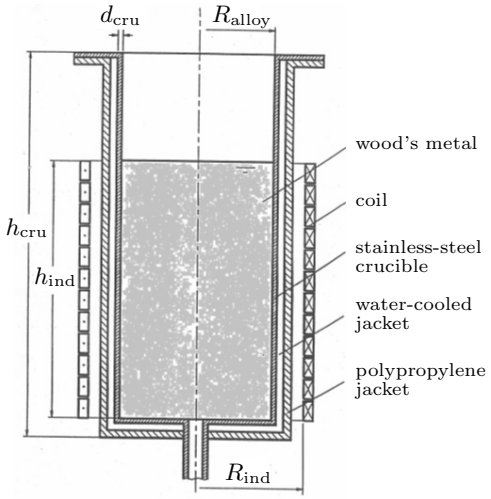

Fig. 1. Geometry and parameters for *big* and *small* laboratory scale ICF setups.

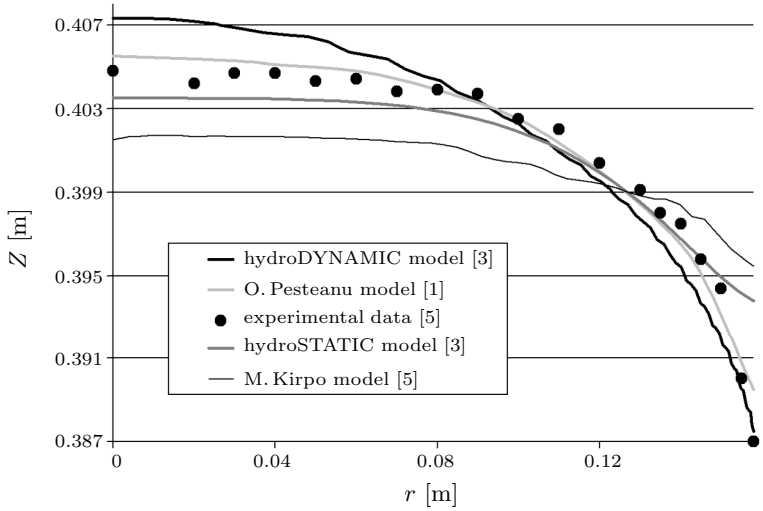

Fig. 2. Comparison of experimental measurements and other models with 2D model calculation results for the steady state meniscus shape in a *big* laboratory scale ICF setup with a precised crucible conductivity.

It was found that overestimation of the crucible conductivity led to an exaggerated EM shielding effect and was the main reason for the smaller height of the calculated meniscus. Recalculation of the quasi-steady state meniscus shape with a proper crucible conductivity of $\sigma_{\mathrm{Fe}} = 1.4 \cdot 10^6\,[\Omega\cdot\,\mathrm{m}]^{-1}$ has succeeded in a better model and experiment agreement (Fig. 2). The height of the meniscus in experiment was 18 mm and the 2D hydrodynamic model predicted 20 mm that made approximately a difference only of 10%. Eventually, the 2D hydrodynamic model has been refined, and a better correlation with the experimental measurements and the model of O. Pesteanu has been obtained.

Despite the nice agreement, the height of the quasi-steady state meniscus in experiment was below 1% both with respect to the melt height and diameter. The experimental data for a more pronounced meniscus remained relevant for proper 2D model verification.

Hence, previously never published experimental measurements for steady state meniscus heights above initial filling (E. Baake, 1992) in a *small* laboratory scale ICF (Fig. 1) were used for the further 2D model verification.

The calculations were performed for an inductor current frequency of 330 Hz ($\delta_{\mathrm{EM}} = 2.8$ cm) and several current values. A fine mesh with a typical element size of 0.3 cm was used for the HD part of the problem.

The calculated quasi-steady state velocity pattern (left) and the Lorentz force density distribution (right), as well as the meniscus shape in contrast to the experimental data on meniscus height above the initial flat free surface are illustrated in Fig. 3. Experimental measurements are marked by black ticks, while the ticks of vertical lines correspond for the given measurement errors due to the turbulence and mean flow instability, which caused the free surface fluctuations.

As it was expected, the enhancing current caused a greater free surface deformation and intensified the flow.

In the calculation (a) with the least inductor current, the meniscus height appears to be 30% lower than the one measured experimentally. The discrepancy, which causes it, is still being investigated, however, for the rest of the calculated series the meniscus height above the initial filling appears to be in good agreement with experiment and below the measurement error.

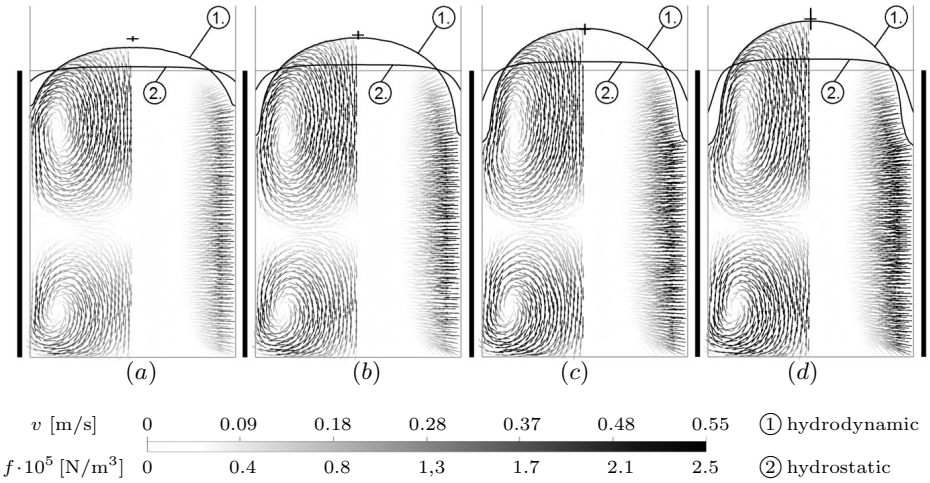

Fig. 3. Quasi-steady state flow pattern (left), Lorentz force density distribution (right) and meniscus shape calculated using 2D hydrodynamic (1) and hydrostatic (2) models in contrast to the experimentally measured meniscus heights above initial filling (black ticks) in a *small* laboratory scale ICF for $f = 330\,\mathrm{Hz}$ and (*a*) $I_{\mathrm{ef}} = 1753\,\mathrm{A}$; (*b*) $I_{\mathrm{ef}} = 2020\,\mathrm{A}$; (*c*) $I_{\mathrm{ef}} = 2262\,\mathrm{A}$; (*d*) $I_{\mathrm{ef}} = 2464\,\mathrm{A}$.

The significance of the flow pattern contribution to the free surface shape is confirmed by a worse hydrostatic meniscus agreement with the experimental measurements and hydrodynamic model calculation (Fig. 2).

2. Application of a 2D model for the case of electromagnetic levitation. In case of EM levitation due to the prominent skin-effect ($\delta_{\mathrm{EM}} = 2.3\,\mathrm{mm}$), large Lorentz forces are distributed in the very narrow melt volume adjoining the free surface. On the other hand, with the VOF technique, it is absolutely normal that the interface is smeared over 2 to 3 mesh elements. For a particular combination of physical phenomena and their numerical treatment, the Lorentz forces appear to be acting on the air adjoining the free surface that causes a non-physical acceleration of the light fraction. Because of the air small density ($\rho_{\mathrm{air}} = 1\,\mathrm{kg/m^3}$), in contrast to the density of the alloy ($\rho_{\mathrm{alloy}} = 9400\,\mathrm{kg/m^3}$), this leads to a dramatic increase of the Courant number and the crash of the whole calculation.

Numerical difficulties were technically solved in the following way. After each series of the coupled HD and EM calculation, the Lorentz force distribution, which corresponds to the new free surface shape, is used as an updated mechanical momentum source, and the initial flow conditions from the previous cycle are used at the beginning of each VOF calculation series. Since the influence of the air motion on the free surface dynamics is negligible, we have the right to stop the air after each Lorentz force recalculation. However, setting the air velocity equal to zero at the beginning of each calculation cycle leads to the interface smearing.

In order to prevent the non-physical interface diffusion, it was proposed to initialize the air velocity field with the melt velocity pattern. This means that in regions, where only one phase exists, the air is initialized with zero velocity, meanwhile, in mesh elements containing both phases the air gains the velocity of the melt. Such technical trick allowed to perform a stable free surface dynamics calculation for the case of 2D electromagnetic levitation.

Copper inductor	
Lower inductor I_{ef}	40 kA, $\varphi = 0$
Upper inductor I_{ef}	24 kA, $\varphi = \pi$
Frequence	50 kHz
Levitating drop	
Alloy density	3400 kg/m^3
Surface tension	0.4 N/m
Dynamic viscosity	0.0042 Pas
Conductivity	10^6 S/m
Initial conditions for drop	
Spherical shape ($r = 4$ mm	Zero velocity

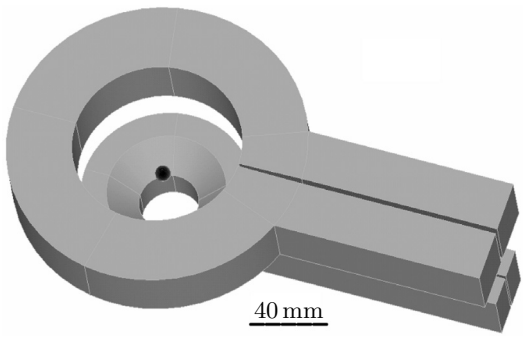

Fig. 4. Geometry and parameters for the numerical experiment on droplet levitation.

A system of two inductor turns and alloy drop under the initial conditions of spherical shape and zero velocity was considered (Fig. 4). The aim of the 2D axisymmetric numerical experiment was to entrap the alloy and obtain a stable levitation. The design of the setup and the operational parameters were not adopted from any experimental data, they were not optimized either, and this is the reason of the exaggerated inductor current values.

A fine timestep of 0.1 ms for the Lorentz force recalculation due to the free surface shape change, as well as a fine space discretization of 0.1 mm both for the EM ($\delta_{\text{EM}} = 2.3$ mm) and the HD calculation was used.

Due to the high inductor frequency, the current induced in the melt is counter-oriented with respect to the primary current in the inductor. By the phase shift of $\phi = \pi$ between the upper and lower inductor turns we ensure the existence of a region in the melt, where the induced currents due to their counter-orientation partially compensated each other. In some respect, the conditions between the upper and lower inductors become similar to the situation on the symmetry axis in the framework of one inductor turn. This leads to formation of regions with a minimum of Lorentz force, where the melt leak is prevented only by a contribution of the surface tension. This means that only slight masses can be levitated in the way described. However, an accurate choice of the physical parameters can ensure a quite stable EM levitation.

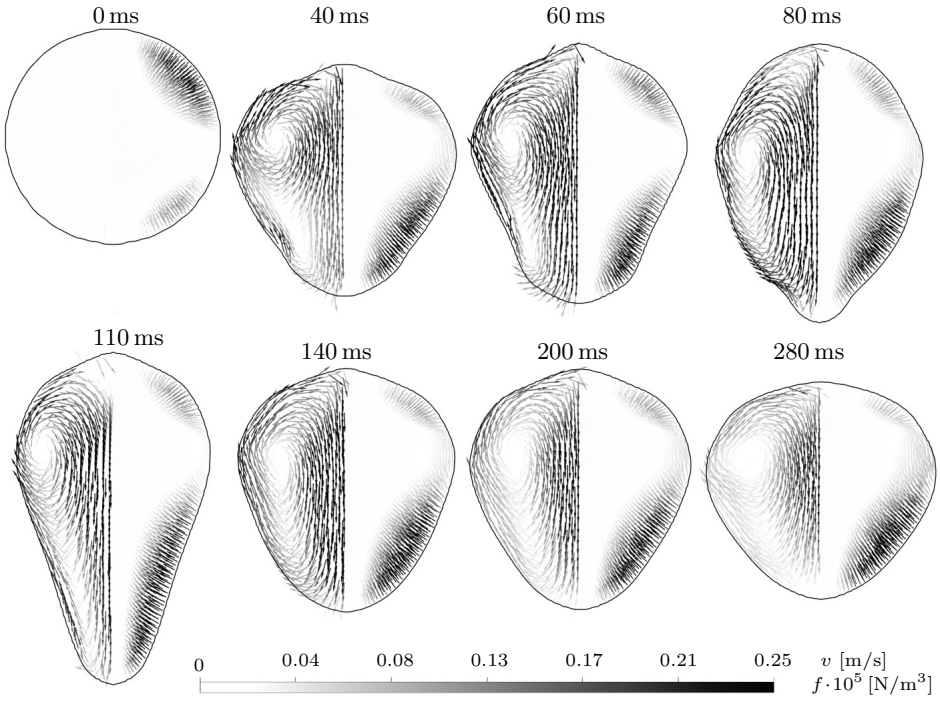

Fig. 5. Instantaneous velocity pattern (left), Lorentz force density distribution (right) and free surface shape of a levitating drop obtained by transient calculation of the 2D hydrodynamic model.

The first calculation results of the levitating drop in 2D axisymmetric consideration have been obtained (Fig. 5).

The Lorentz force density distribution at $t = 0$ illustrates the Lorentz force singularity on the symmetry axis as well as the Lorentz force minimum on a certain circle of the latitude at the surface due to the phase shift π between the upper and lower inductor turns.

Initial disbalance between gravity and EM forces makes the drop move downwards for the first 40 ms of calculation. The laminar flow (Re = 700) rapidly develops, and one torroidal vortex with a downward velocity is generated on the drop symmetry axis. During the vortex formation, the drop stretches twice in the axial direction, however, reaching the quasi-steady state at $t = 200$ ms, the free surface gains a characteristic "spinning-top" shape and the axial and radial dimensions remain comparable.

By tracing the free surface point oscillations on the symmetry axis and oscillations of the melt drop barycenter (Fig. 6), it can be concluded that for the rest of the calculation time the barycenter slightly oscillates around the steady state location. Meanwhile, the free surface point on the top of the drop oscillates with a high frequency and a small amplitude, whereas, the bottom point performs slow fluctuations of big amplitude.

The free surface region on the top of the drop corresponds to the torroidal vortex flow collision, and free surface instabilities of small relaxation times are

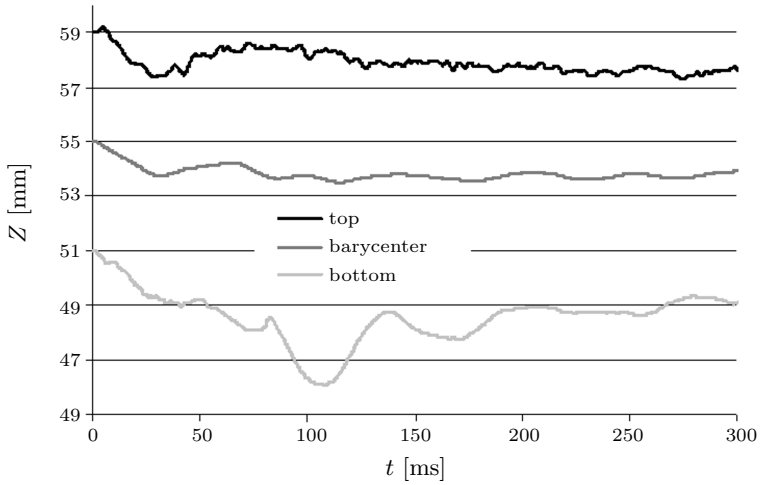

Fig. 6. Free surface top and bottom point oscillations on the symmetry axis and oscillations of the melt drop barycenter.

expected here. The fluctuations of the bottom point are determined by all flow conditions, where greater masses are involved. However, we should be cautious in providing physical interpretation because the numerical effect contribution to the symmetry axis region has not been yet investigated.

Despite a step towards the development of the approach, some difficulties still remain unresolved.

For larger surface tension coefficients, the conservation of mass is not ensured with sufficient precision, presumably, for the following reason. In the framework of one element, the isoline of constant volume fraction is represented as a straight line and the free surface − as a polygon. Prominent polygon fractures form singularities with a great surface tension force that leads to large instantaneous velocities normal to the free surface. This increases the Courant number more than unity and leads to a worse mass conservation.

Possible problem solutions are being considered because the studied parameter (surface tension, inductor frequency, ect.) are of great interest for such physical phenomena.

Experimental verification of the free surface dynamics model applied for the case of EM levitation provides the further plans of research.

3. Formulation of the 3D model. Experimental monitoring of the HD movement of the melt and free surface dynamics evidenced on the lack of axial symmetry in the physical process. This means that the 2D model formulation with the forbidden azimuthal heat and mass transfer provides a priori incomplete results. The formulation of a coupled full 3D hydrodynamic and 3D electromagnetic calculation of the free surface dynamics of the melt in the induction crucible furnace assures the further step of research.

The same as in 2D axially symmetric consideration, the numerical calculation is arranged via ANSYS Classic for 3D EM calculation, ANSYS/CFX for 3D HD VOF calculation and their external coupler. Schematical calculation arrangement is presented in Fig. 7.

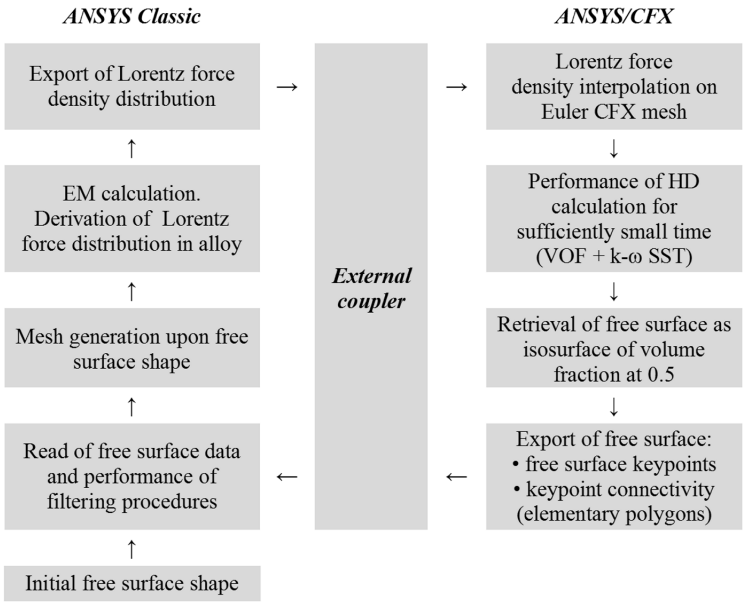

Fig. 7. Schematic presentation of 3D calculation arrangement for free surface dynamics.

The initial free surface shape (flat free surface) as well as every transient state of the meniscus shape obtained from the VOF calculation is saved in a file. The file contains free surface keypoint numbers n_i, keypoint coordinates (x_i, y_i, z_i), and series of elementary keypoint connectivities, whereas the connectivities are named as sequences of keypoint numbers that indicate the order of free surface keypoint line connection for definition of elementary polygons.

Transferring the free surface keypoints and elementary polygons from CFX to ANSYS Classic, a self-written filtering procedure is performed in order to avoid generation of degenerate surface elements, which cause errors in the ANSYS Classic volume mesher. This procedure is focused mainly on close keypoint merging, polygon reconstruction and further decomposition to maximally equilateral triangles.

The HD calculation in CFX is performed on the fixed Euler mesh containing prisms. In the range of one element, the free surface is presented as a plane. As a result of the hexahedron intersection with the plane, elementary polygons consisting of 3 to 6 edges are expected. For instance, cutting hexahedron with a plane at a small angle along the edge derives such degenerate polygon with edges that have a difference of several orders in length.

By the end of filtering, a free surface consisting of elementary triangular non-degenerate areas is obtained, and a mesh for EM calculation is generated. It must be mentioned that the spiral inductor in the electromagnetic part of the problem is considered as 11 separate turns with gaps for application of electromagnetic boundary conditions (Fig. 8). This gap introduces a slight artificial axial asymmetry into the Lorentz force distribution and, as a result, influences the flow pattern and meniscus shape.

By the end of the EM calculation, the Lorentz force density is retrieved and interpolated on the mesh for the HD calculation. Using the flow pattern and meniscus shape from the previous cycle as initial conditions, a transient HD calculation is performed for a sufficiently small time interval. Later, the isosurface of

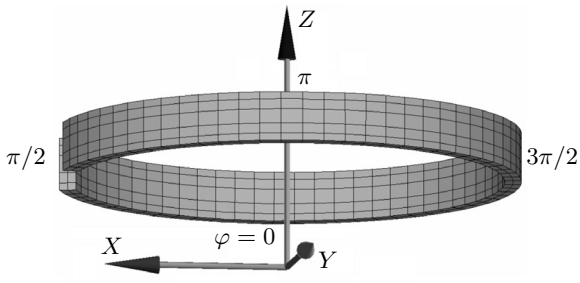

Fig. 8. Inductor turn with a gap at $\phi = \pi/2$ for EM boundary conditions.

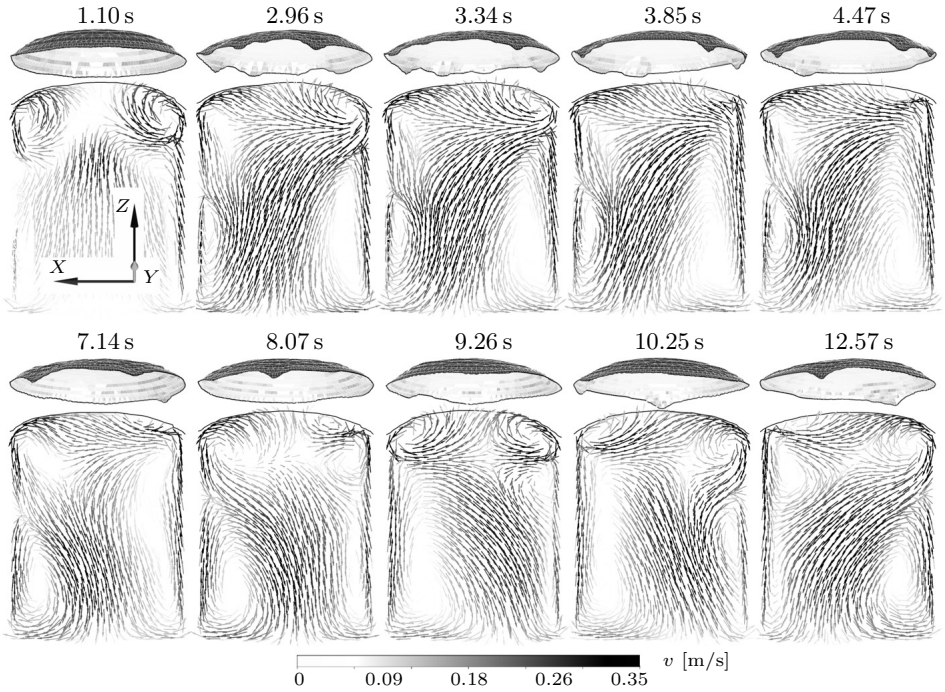

Fig. 9. Instantaneous velocity patterns on the XZ plane and free surface shapes obtained by a 3D hydrodynamic model transient calculation at $I_{\text{ef}} = 3\,\text{kA}$ and $f = 385\,\text{Hz}$.

the volume fraction representing the free surface is saved in a file. After that the whole calculation cycle is repeated.

4. 3D model calculation results. On the basis of the *big* laboratory scale ICF experimental setup (Fig. 1) with a crucible inner radius of 15.8 cm and 70% melt filling with respect to the inductor height and applying an effective inductor current of $I_{\text{ef}} = 3\,\text{kA}$ at the frequency $f = 385\,\text{Hz}$, the free surface dynamics for the first 14 s of flow is calculated.

The instantaneous velocity patterns on the XZ cross-section, where the flow assymetry due to the inductor gap is pronounced, and the free surface shapes, shifted upwards for convenient representation, illustrate the dynamics of the process (Fig. 9).

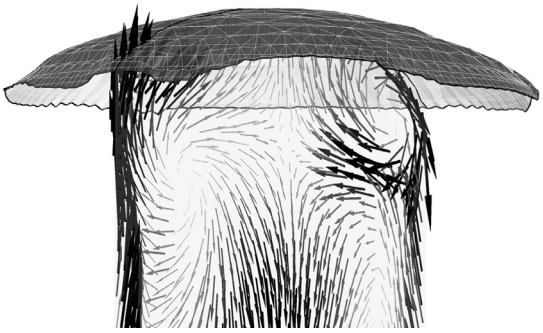

Fig. 10. HD flow asymmetry leads to upward flow along the walls and causes free surface perturbations, which are very pronounced on the meniscus perimeter. The velocity pattern corresponds to $t = 2.2\,\mathrm{s}$ of the flow time.

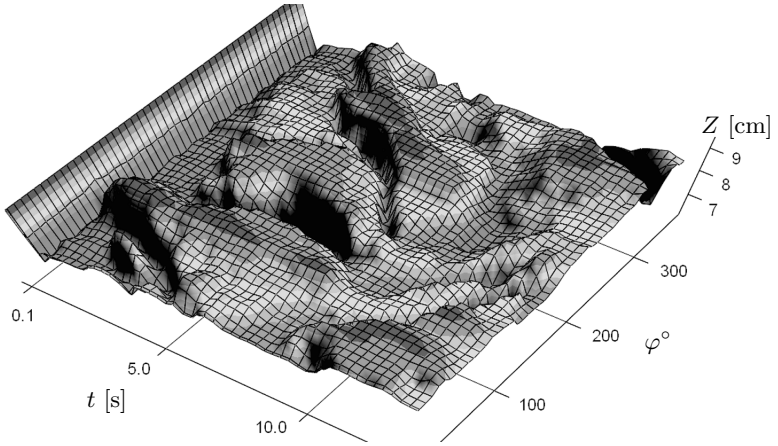

Fig. 11. Heights of free surface perimeter points as a function of the azimuthal angle ϕ and time t obtained in calculation with $I_{\mathrm{ef}} = 3\,\mathrm{kA}$ and $f = 385\,\mathrm{Hz}$.

In 1 second the flow achieves the quasi-steady state and it can be observed that the meniscus height above initial filling and the meniscus shape, in general, remain steady. However, the instability of hydrodynamic flow (Fig. 10) leads to continuous reallocation and deformation of two torroidal vortices. This causes a redistribution of the dynamic pressure on the free surface, which leads to a free surface strain. Meanwhile, due to the skin effect ($\delta_{\mathrm{EM}} = 2.6\,\mathrm{cm}$), the Lorentz forces are distributed in a narrow volume of the melt next to the crucible. A slight change of the free surface shape in the crucible wall region has a rapid effect on the Lorentz force distribution and the flow pattern.

With reference to the results of numerical calculation, such reciprocal interaction leads to development of free surface perturbations, which travel along the crucible wall and are in qualitative agreement with experimental observations [5]. The dynamics of these perturbations is clearly notable from the plot of the meniscus perimeter point heights as a function of time and azimuthal angle ϕ (Fig. 11).

A prominent motionless ($\phi = 90°$) and long living ($0.1\,\mathrm{s} < t < 10\,\mathrm{s}$) perturbation caused by the smaller electromagnetic pressure is located right next to the inductor gap. One highly marked travelling perturbation is traced at $250° < \phi < 360°$ during $0.1\ \mathrm{s} < t < 10\,\mathrm{s}$. Another two hollows travel at $80° < \phi < 220°$ during $10\,\mathrm{s} < t < 15\,\mathrm{s}$.

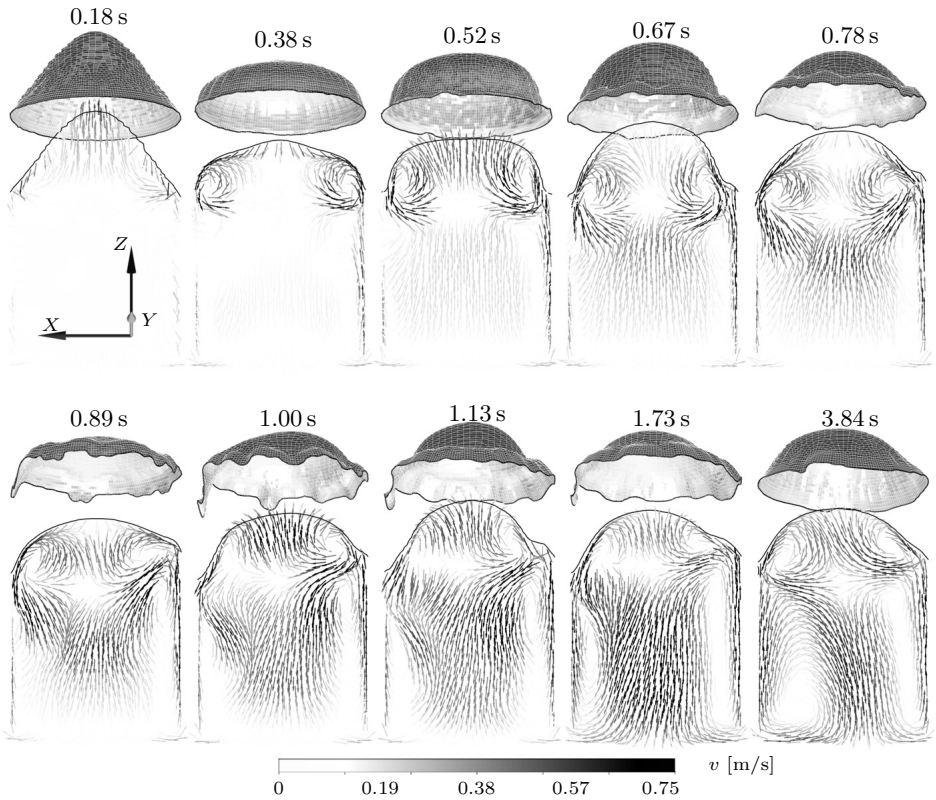

Fig. 12. Instantaneous velocity patterns on the XZ plane and free surface shapes obtained by 3D hydrodynamic model transient calculation at $I_{\text{ef}} = 5\,\text{kA}$ and $f = 385\,\text{Hz}$.

Presumably, the mentioned above inductor gap introduces the symmetry plane that has the tendency to absorb the azimuthal propagation of the free surface perturbations. Therefore, a calculation with a more realistic spiral inductor is of great interest.

The calculation for the first 4 seconds of flow with an enhanced inductor current of $I_{\text{ef}} = 5\,\text{kA}$ at the same frequency $f = 385\,\text{Hz}$ is performed and instantaneous velocity patterns on the XZ cross-section as well as free surface shapes are presented in order to sketch the dynamics of the process (Fig. 12).

As expected, a stronger inductor current initiates a stronger free surface perturbation and the quasi-steady state meniscus height and intensifies the flow as well. The introduced axial asymmetry in Lorentz force distribution due to the inductor gap in electromagnetic calculation is insignificant for the initial process development. However, at $t = 0.8\,\text{s}$ the asymmetry in flow and free surface shape becomes clearly notable.

Let us remind that for the small amplitude free surface oscillations in the *big* laboratory scale ICF geometry with filling of 70 was estimated as $T_{\text{theor}} = 0.41\,\text{s}$ [3]. Good agreement below 5% between the analytical estimation and the calculation results for the free surface oscillation period on the symmetry axis is obtained. It was mentioned previously that the starting flow development and the free surface dynamics appeared to be axisymmetric in a 3D case, and, as a result,

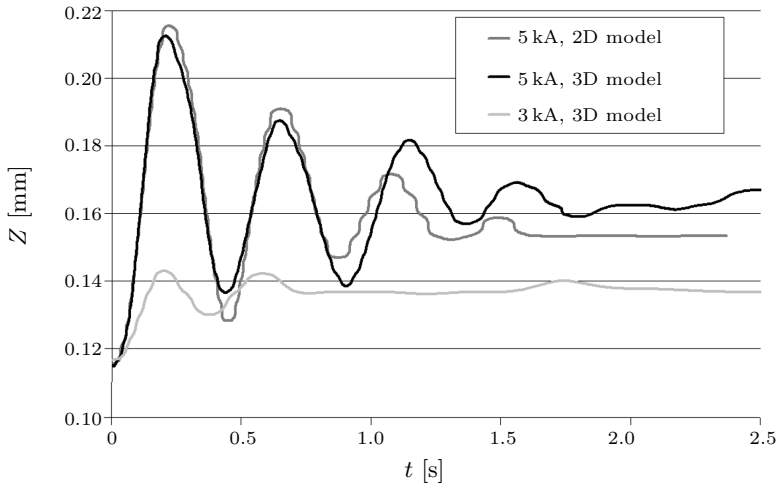

Fig. 13. Oscillations of free surface points on the symmetry axis in a *big* laboratory scale ICF with $f = 385$ Hz.

a good correlation between the first two free surface oscillations in 2D and 3D consideration is achieved (Fig. 13).

5. Conclusions.

• Better agreement between the two-dimensional model calculation results and the experimental measurements for the steady state meniscus shape in a *big* laboratory scale ICF was achieved with account of a precised crucible electrical conductivity value. The comparison of the experimental measurements for pronounced meniscus heights above initial filling in a *small* laboratory scale ICF and the two-dimensional model calculation results has approved the model accuracy.

• By means of the approach modification, a step forward was made in application of the two-dimensional model for the case of electromagnetic levitation. The first calculation results are obtained and the model verification is on top of the day. Difficulties with volume conservation in the case of greater surface tension must be solved in order to perform parameter studies that are of great interest.

• The free surface oscillation period obtained using the developed two-dimensional and three-dimensional models is in good agreement with the analytical estimation, however, the experimental data for free surface dynamics remains relevant.

• Three-dimensional calculation results of free surface dynamics reveal an interesting phenomenon of free surface wave propagation along the crucible wall. Considering the spiral inductor and applying the LES turbulence description with finer time and space discretization provide the further step in research and must lead to valuable physical results.

6. Acknowledgements. The study was performed under the financial support of the ESF project at the University of Latvia; contract

No. 2009/0223/1DP/1.1.1.2.0/09/APIA/VIAA/008

and

2009/0162/1DP/1.1.2.1.1/09/IPIA/VIAA/004.

REFERENCES

[1] O. Pesteanu, E. Baake. The multicell volume of fluid (MC-VOF) method for the free surface simulation of MHD flows. *ISIJ International*, vol. 51 (2011), pp. 707–721.

[2] V. Bojarevics, K. Pericleous. Modelling of electromagnetically levitated liquid droplet oscillations. *ISIJ International*, vol. 43 (2003), pp. 890–898.

[3] S. Spitans, A. Jakovics, E. Baake, B. Nacke. Numerical modeling of free surface dynamics of conductive melt in the induction crucible furnace. *Magnetohydrodynamics*, vol. 46 (2010), pp. 317–328.

[4] F. Hegewaldt, L. Buligins, A. Jakowitsch. Transient bath surface bulging at energization of an induction-type crucible furnace. *Elektrowärme international*, vol. 51 (1993), no. B1, pp. 28–42.

[5] M. Kirpo. *Modeling of turbulence properties and particle transport in recirculated flows* (Ph.D. thesis, University of Latvia), 2008.

Received 19.11.2011